On the Processing of Bubble Chamber Tracks by Means of In-Line Filtered Holography*

Kazumi MURATA**
Hirofumi FUJIWARA**
Toshimitsu ASAKURA**

(Received September 2, 1968)

Abstract

Some fundamental problems for the application of an in-line Fraunhofer holographic technique to the recording of the bubble chamber tracks were studied. Optical spatial filtering based on the double diffraction method was combined with the recording and reconstructing processes of the bubble chamber holography in order to suppress undesirable beam tracks. Experimental studies were conducted using simulated conditions of bubble chamber tracks and actual bubble-chamber photographs. The results showed some promise of success for using the in-line Fraunhofer holography to bubble chamber photography.

1. Introduction

In the process of recording bubble tracks, the use of holographic techniques was suggested by Welford[1] and Ward and Thompson[2]; the former investigator mentioned the possibility of increasing the focal depth by means of holography and the latter workers proposed an in-line Fraunhofer holography for recording bubble tracks. After bubble chamber photographs are taken, other difficulties arise in the automatic scanning and measuring of the films. To solve this problem the optical computer method was proposed by Falconer[3] for the background of undesirable beam tracks. An application of the in-line Fraunhofer holography for bubble chamber photographs is reported in this paper in which the construction of an in-line filtered hologram is proposed to suppress undesirable beam tracks in the hologram-recording process. Theoretical and experimental work on the in-line Fraunhofer holographic method has already been conducted by Thompson and others[4]. Compared against the two-beam interferometric hologram method, the present method has certain advantages related

* The present paper was reported at the US-Japan Seminar on Holography held in Tokyo (October, 1967).

** Department of Applied Physics, Faculty of Engineering, Hokkaido University, Sapporo, Hokkaido, Japan.

to film resolution, exposure time, temporal coherence and mechanical stability.

2. Basic Theory

The basic theoretical derivation of the in-line Fraunhofer hologram process was given in detail by Thompson and others. The principle was summarized and discussed in this section, and extended to the case of the two close objects.

The in-line Fraunhofer hologram is confined to a situation where the far-field condition is satisfied for individual objects while the entire sample volume remains in the near-field. In such a case it is obvious that if the extent of the background plane wave is much larger than the object, it then proceeds as a plane wave to the receiving plane. Thus, for a coherent background we bave,

$$a_r(x_2) = e^{ikz_1}, \qquad k = 2\pi/\lambda. \tag{1}$$

Here we assume that the plane wave has been transmitted without absorption through the sample volume. Now, let us consider the Fraunhofer diffraction produced by the objects. The reduced form of Huygens' principle states that the amplitude distributions $u(x_1)$ and $a_0(x_2)$ are related through the equation

$$a_0(x_2) = -\frac{ik}{2\pi}\int u(x_1)\frac{e^{ikr}}{r}\,dx_1. \tag{2}$$

Assuming now that the size of the objects is small enough as compared with the distance z_1 of the two planes. Hence we need only to maintain terms up to the second for the expansion of r, thus we can write

$$r = \left\{z_1^2 + (x_1 - x_2)^2\right\}^{1/2} = z_1 + \frac{x_2^2}{2z_1} - \frac{x_2 x_1}{z_1}. \tag{3}$$

Inserting this into Eq. (2) and noting $z_1 \gg x_1^2/\lambda$, we have for Eq. (2)

$$a_0(x_2) = -\frac{ik}{2\pi}\frac{e^{ikz_1}e^{i\frac{kx_2^2}{2z_1}}}{z_1}\int u(x_1)e^{-i\frac{kx_2x_1}{z_1}}\,dx_1 = -\frac{ik}{2\pi}\frac{e^{ikz_1}e^{i\frac{kx_2^2}{2z_1}}}{z_1}\tilde{u}(x_2) \tag{4}$$

where $\tilde{u}(x_2)$ is the Fourier transform of the object. By combining the Fraunhofer diffraction pattern (4) with a coherent background (1) the recorded intensity across the x_2 plane can now be written as

$$\begin{aligned} I(x_2) &= |a_r(x_2) + a_0(x_2)|^2 \\ &= 1 + \frac{k^2}{4\pi^2 z_1^2}\left|\tilde{u}(x_2)\right|^2 + \frac{k}{\pi z_1}\tilde{u}(x_2)\sin\left(\frac{kx_2^2}{2z_1}\right) \end{aligned} \tag{5}$$

where we assume that the object is real $[u(x_1) = u^*(x_1)]$. This expression (5) is called an in-line Fraunhofer hologram. The amplitude transparency of the Fraunhofer hologram for a line object (line width $=2b$) is, after properly controlling the gamma (γ) of the photographic process, given by

$$t(x_2)=1+\frac{\gamma kb}{\pi z_1}\left[\frac{\sin\left(\frac{2\pi b x_2}{\lambda z_1}\right)}{\left(\frac{2\pi b x_2}{\lambda z_1}\right)}\right]\sin\left(\frac{k x_2^2}{2z_1}\right). \tag{6}$$

In deriving Eq. (6), the second term in Eq. (5) has been neglected since it is generally very small compared with the other two terms. The film record (6) of the Fraunhofer hologram is a pattern similar to an one-dimensional Fresnel zone plate. Amplitude transmission varying as a constant plus $\sin(kx^2/2z_1)$ exhibits focusing properties with a focal length z_1 and does not produce a degradation effect arising from a virtual image in the Fraunhofer hologram although this effect is present in the Fresnel hologram first proposed by Gabor[5]. An interesting point of the in-line holography is the reconstruction, with a large focal depth, of three-dimensional bubble tracks. As seen in Eq. (6), z information is recorded in the fringe pattern on the hologram so that the two line object at different distances z_1 and z_2 can create their own characteristic zone plates. In the reconstruction process each has their own focusing planes.

We now proceed to consider the hologram for an object of two lines which are situated closely to each other. Following the previous method in the derivation of Eq. (5) by means of Eqs. (1) and (4), we have the recorded intensity across the plane x_2 for this object which is written as

$$\begin{aligned}I(x_2)&=\left|e^{ikz_1}-\frac{ik}{2\pi}\frac{e^{ikz_1}e^{i\frac{kx_2^2}{2z_1}}}{z_1}\tilde{u}(x_2)-\frac{ik}{2\pi}\frac{e^{ikz_1}e^{i\frac{k(x_2+\Delta x)^2}{z_1}}}{z_1}\tilde{u}(x_2+\Delta x)\right|^2\\&=1+\frac{k^2}{4\pi^2 z_1^2}\left\{|\tilde{u}(x_2)|^2+|\tilde{u}(x_2+\Delta x)|^2\right\}\\&\quad+\frac{k}{\pi z_1}\left\{\tilde{u}(x_2)\sin\left(\frac{kx_2^2}{2z_1}\right)+\tilde{u}(x_2+\Delta x)\sin\left(\frac{k(x_2+\Delta x)^2}{2z_1}\right)\right\}\\&\quad+\frac{k^2}{2\pi^2 z_1^2}\tilde{u}(x_2)\tilde{u}(x_2+\Delta x)\cos(2x_2\Delta x).\end{aligned} \tag{7}$$

Here Δx is the distance between the two lines and $(\Delta x)^2$ is neglected in the derivation process of Eq. (7) since Δx is extremely small. Comparing this equation with Eq. (6) we note that the fourth term is added which represents interference between diffracting waves from the two close lines but does not have focusing properties. Furthermore, since the cosine function depends upon

Δx it varies more slowly than $\tilde{u}(x_2)$ when the object distance Δx becomes very small, thus producing interference fringes of comparatively large periods. In addition, this term is inversely proportional to z_1^2 as in the second term so that it is small compared with the third term which is dominant and plays the main role in the reconstruction process. Thus we can conclude that, even though interference phenomena are present between diffracting waves from each object, the fourth term does not have much influence on the reconstruction of the two close objects. So the resolution may be excellent in the in-line Fraunhofer holography.

We now return to Eq. (6) which is the intensity distribution of the hologram made by collimated light and we shall consider it in detail. The second term of Eq. (6) consists of three factors: a constant factor, a Fraunhofer diffraction factor, and a focusing factor. The factor $(kb/\pi z_1)$ is a constant depending only upon the developing process. The second factor is the Fraunhofer diffraction pattern of the object. The third factor $\sin(kx_2^2/2z_1)$ is the Fresnel zone term which is considered as a focusing term necessary for the reconstruction of the original object. The second and third factors are very important for the hologram. The multiplication form between these two factors indicates that the third factor $\sin(kx_2^2/2z_1)$ is amplitude-modulated by the factor $\mathrm{sinc}(2\pi bx_2/\lambda z_1)$. Now let us consider the following cases,

$$\begin{aligned} &\sin\left(\frac{2\pi bx_2}{\lambda z_1}\right)=0 \longrightarrow x_2=\frac{\lambda z_1}{2b}n \\ &\sin\left(\frac{\pi x_2'^2}{\lambda z_1}\right)=0 \longrightarrow x_2'=\sqrt{\lambda z_1 n'}\ . \end{aligned} \tag{8}$$

The last equation indicates that the Fraunhofer hologram has the same properties with the Fresnel zone plate as a focusing factor. The number of interference fringes within the first minimum on the diffraction pattern of the object can be obtained by

$$\frac{x_2(n=1)}{x_2'(n'=n')}=\frac{\sqrt{\lambda z_1}}{2b}\frac{1}{\sqrt{n'}}=1 \qquad \therefore \quad n'=\frac{z_1}{\dfrac{|2b|^2}{\lambda}}\ . \tag{9}$$

This result is nothing but the Fraunhofer condition $|2b|^2/\lambda \ll z_1$. That is, the Fraunhofer condition $n'\gg 1$ means that large numbers of fringes must be present within the first minimum of the diffraction pattern of the object. In other words, as long as the amplitude modulation of the Fresnel zone term $\sin(kx_2^2/2z_1)$ is small, the image can be faithfully reconstructed. If the width of the object becomes very narrow and approaches the delta function, the amplitude of the Fresnel zone term may be finally modulated only by the transfer function of the film. Therefore, the reconstructed image becomes equal to the spread function of the film and the resolution limit of the in-line holography is only dependent upon film resolution. On the other hand, the width of interference fringes in the in-line Fraunhofer holography is much larger than that in the conventional two-beam interferometric method, so that a relatively low resolution film may be useful for recording the Fraunhofer hologram. Consequently, special care for the film of the hologram recording is not necessary.

3. Filtered Hologram

Based on the above considerations, a preliminary experiment was performed. Figure 1 shows the schematic diagram of the experimental setup where a He-Ne gas laser was used as the coherent light source. In Fig. 2, the actual arrangement of this setup is shown. A collimator provides a coherent plane wave to illuminate a sample volume where a bubble chamber or other simulated objects such as wires and glass fibers were used. After passing through the sample volume, the coherent light is focused on the diffraction plane where the Fraunhofer diffraction pattern (spectrum) is produced. This

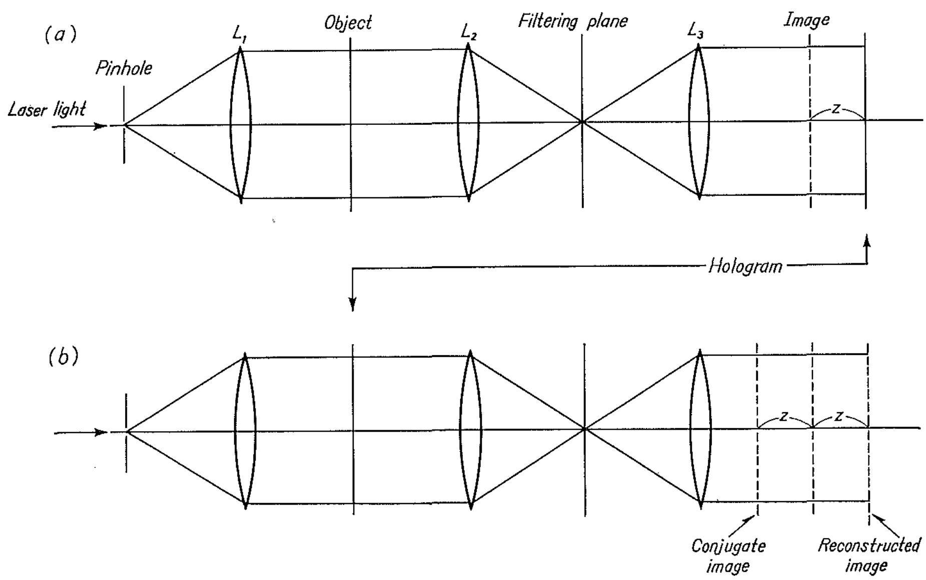

Fig. 1. Schematic diagram of an optical system for the in-line filtered Fraunhofer holography. (a) Recording of the hologram. (b) Reconstruction from the hologram.

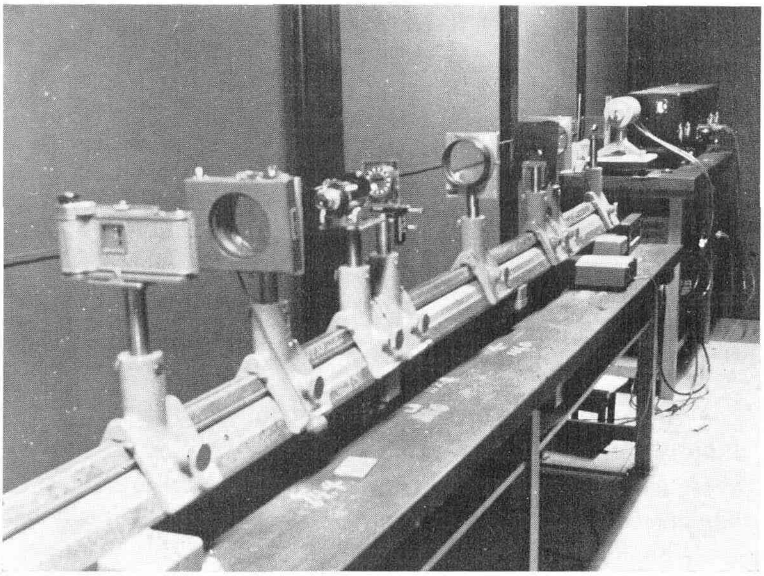

Fig. 2. Arrangement of the in-line filtered Fraunhofer holography using a simulated bubble chamber.

plane is called the filter plane which contains an opaque mask to suppress undesirable beam tracks. The mask cuts out the spectrum of undesirable tracks but passes a zero-order spectum and spectra of desirable tracks which together produce the zone-like interference fringes. Since the undesirable tracks in a bubble chamber are usually all parallel, their spectra are formed at the spectrum plane in a direction perpendicular to the undesirable tracks. The pattern without undesirable spectra is a filtered hologram. At the spectrum plane the line opaque mask with a hole in the center is usually employed to suppress the undesirable spectra. In the reconstruction process (see Fig. 1), the same setup was used where the hologram was placed at the object plane and then the reconstructed image was produced at the original hologram plane.

The method stated above is a case where optical spatial filtering was used in the recording of the hologram. However, this filtering technique of suppressing undesirable beam tracks can also be useful in the reconstruction from the hologram. In this case, spatial filtering could be conducted at the Fourier-transform plane of the hologram.

4. Experimental Results

Now let us show the experimental results for the in-line filtered holography.

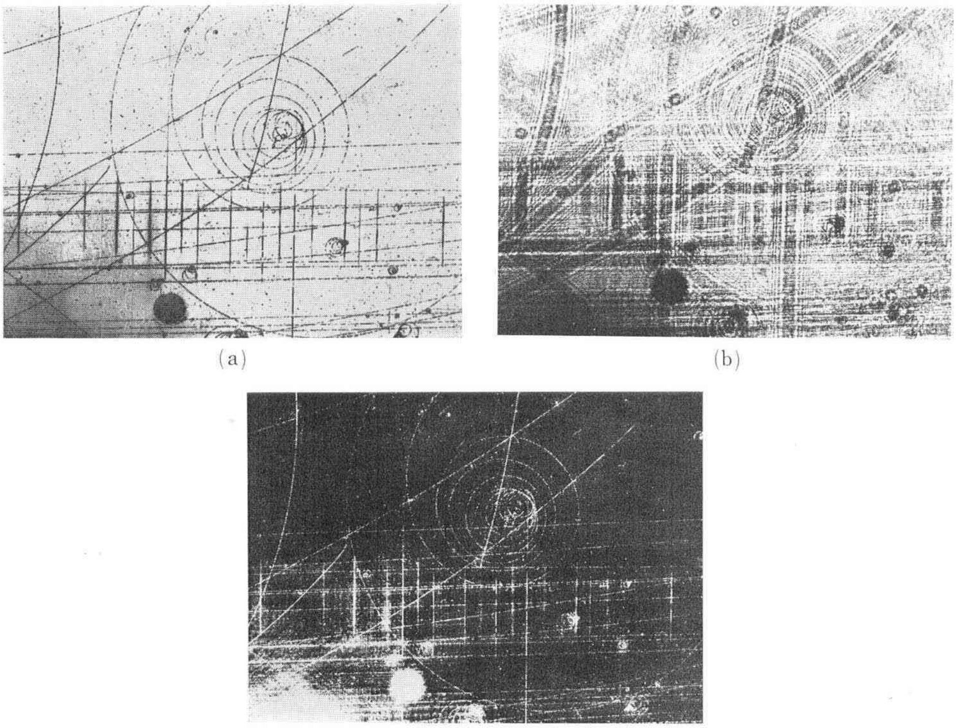

(a) (b) (c)

Fig. 3. (a) Bubble chamber photograph, (b) hologram at $z=20$ cm without filtering, and (c) reconstruction from the hologram.

Figure 3 (a) shows an actual bubble chamber photograph used as an object, while Figs. 3 (b) and (c) are the hologram without filtering and the reconstructed image thereof, respectively. The reconstruction is extremely excellent without the usual deterioration of the virtual image present in the Fresnel hologram. These figures indicate that, although interference appears among diffracting waves from each line object, the reconstruction of the original lines is almost complete. In Fig. 4 (a), however, the filtered hologram of the bubble chamber photograph is shown where the horizontal parallel lines are suppressed on the hologram-recording process. Figure 4 (b) indicates its reconstructed image. On the other hand, Figs. 4 (c) and (d) show the filtered hologram and its reconstructed image, respectively, where the vertical parallel lines are suppressed as undesirable beam tracks.

In order to see various properties of the in-line filtered Fraunhofer hologram in closer detail, we used simulated objects consisting of wires and glass fibers. Figure 5 (a) shows the filtered hologram of an object which consists

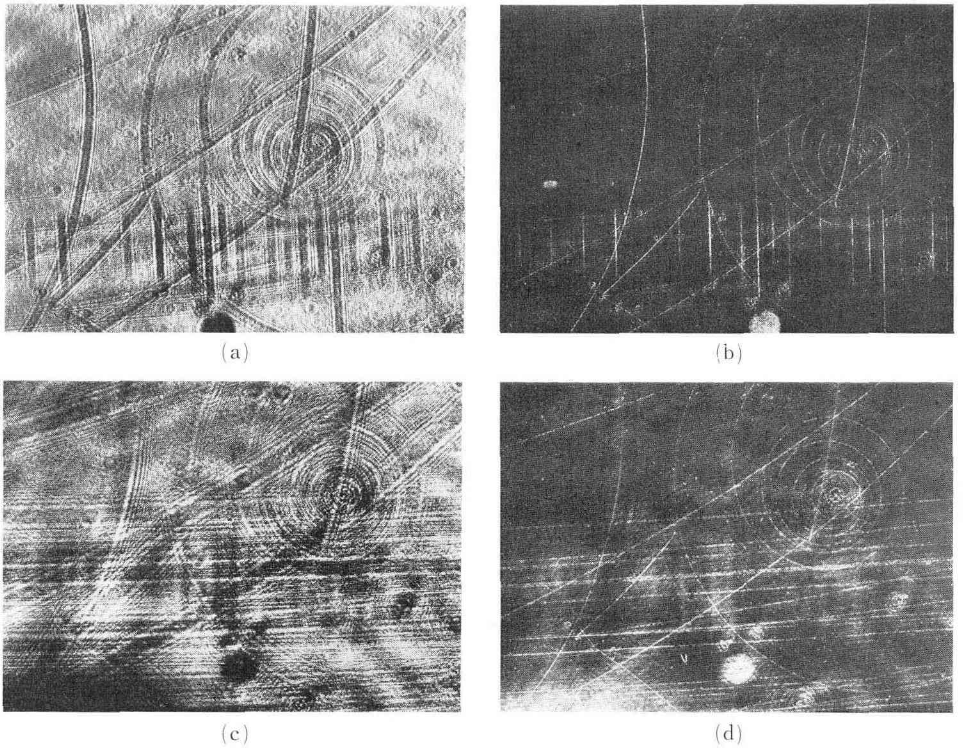

(a) (b) (c) (d)

Fig. 4. (a) Hologram of the bubble chamber photograph at $z=10$ cm with spatial filtering on the horizontal beam tracks, and (b) reconstructed image of the desirable event tracks. (c) Hologram of the same object at $z=30$ cm with filtering on the vertical lines, and (d) reconstruction from the filtered hologram.

of six horizontal and one vertical lines (central lines are made of glass fiber). Here the hologram was made in the plane defocused 10 cm from the conjugate image plane. Figures 5 (b) is the reconstructed image where the vertical line alone is filtered-out as an undesirable track although it still appears as a blurred image and consequently has no ability of faithfully reconstructing the original object. Figures 5 (c) and (d) show the filtered hologram recorded at a 30 cm out-of-focus plane and the reconstructed image.

Reconstructed images can be improved by decreasing the diameter of the central hole in the mask passing the zero-order spectrum. This point will be shown in the following figures. The object consists of two vertical and two horizontal lines. In the following three cases, the vertical lines were omitted as undesirable tracks. Figure 6 (a) shows the filtered hologram for which a mask having a 2.6 mm diameter of the hole passing the zero-order spectrum

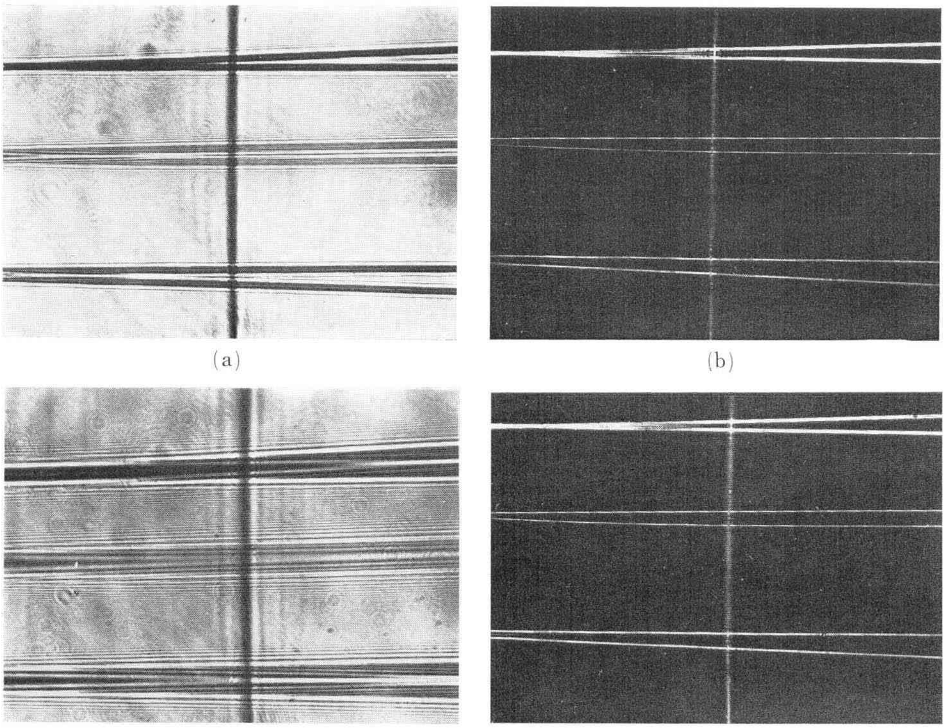

(a) (b) (c) (d)

Fig. 5. (a) Hologram of the five wires (higher two lines, 0.16 mm ϕ; lower two lines and a vertical line, 0.10 mm ϕ) and of the central two 0.05 mm ϕ glass fibers in one plane at $z=10$ cm with filtering on the vertical line, and (b) reconstructed image of these wires and glass fibers. (c) Hologram of the same object made at $z=30$ cm with filtering on the vertical line, and (d) reconstructed image from the filtered hologram.

is used. Figure 6 (b) is the reconstructed image. In this case, the filtering effect was not seen owing to the relatively large diameter of the hole. Now we proceed to reduce the diameter of the zero-order passing hole. Figure 6 (c) indicates the hologram made by using a mask with a 0.6 mm diameter hole. Its reconstructed image is shown by Fig. 6 (d) from which it is seen that the filtering effect begins to appear since the image of the vertical lines is fairly diminished. An excellent filtered hologram was found by using a mask with a 0.35 mm ϕ hole and is shown in Fig. 6 (e). The reconstructed image is also excellent as seen in Fig. 6 (f) in which the vertical lines almost completely disappear. Thus it was concluded that, in order to obtain a well filtered hologram, it is necessary to pay special attention to the filtering opaque mask,

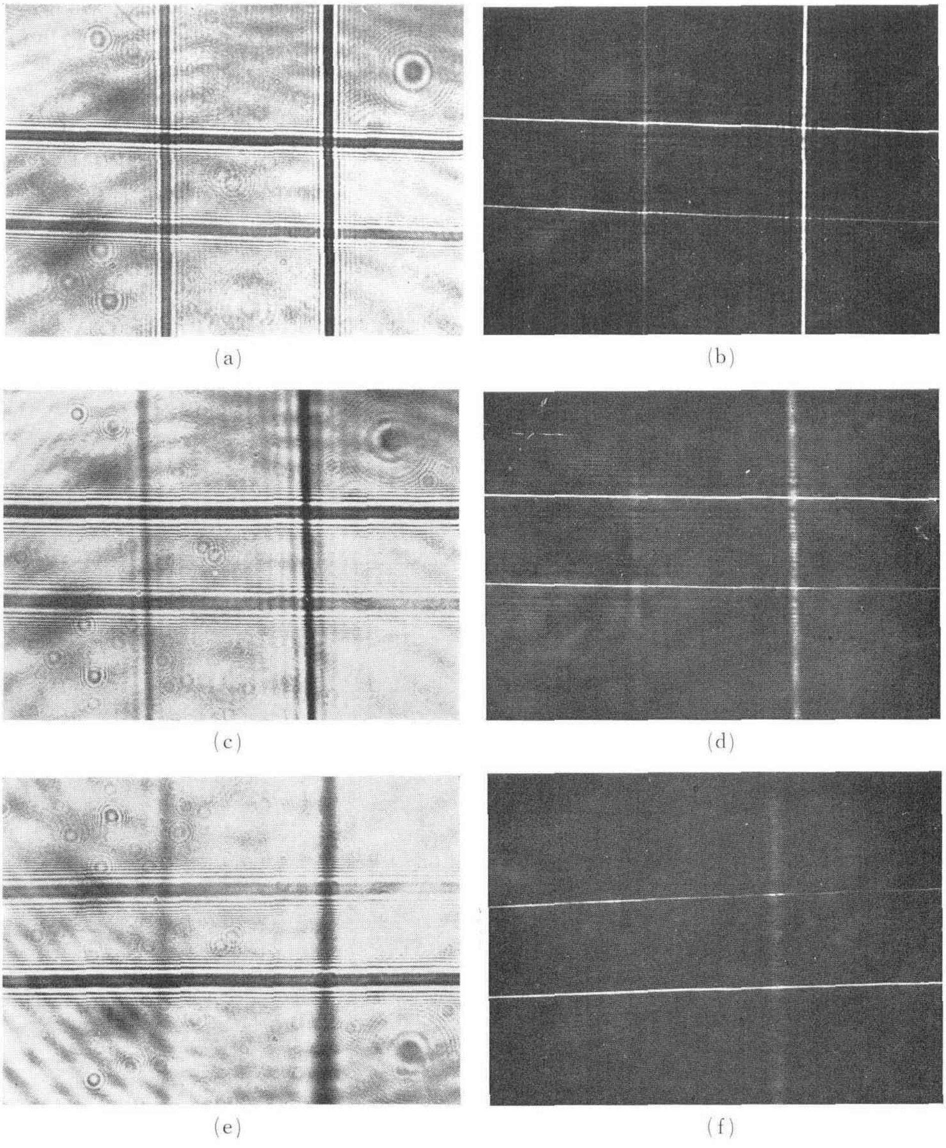

Fig. 6. (a) Hologram made by using a mask of a zero-order passing hole having a 2.6 mm diameter (the width of the mask = 1.5 mm) with filtering on the vertical lines, (b) reconstructed image from the hologram. (c) Filtered hologram with the mask of the 0.6 mm ϕ hole, and (d) image from the filtered hologram. (e) Filtered hologram with the mask of the 0.35 mm ϕ hole, and (f) reconstructed image from the filtered hologram.

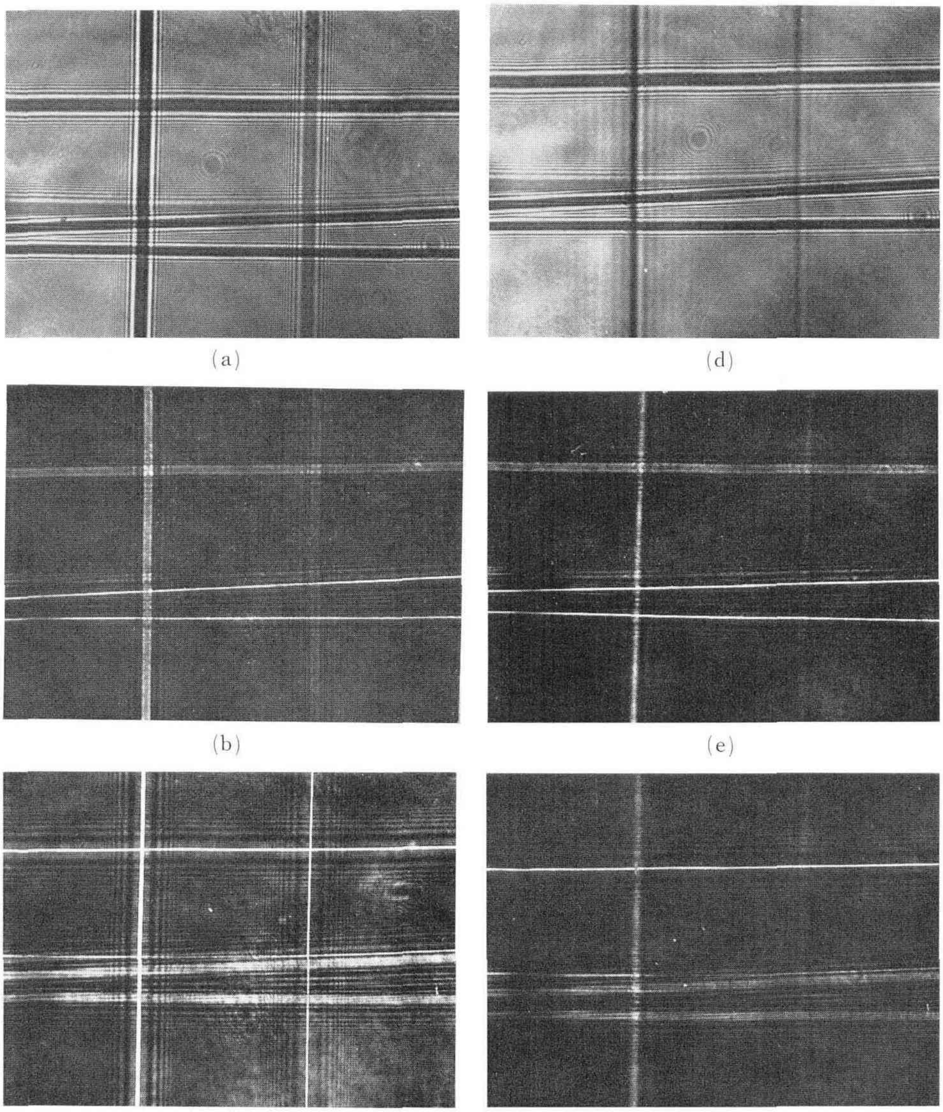

(a) (d) (b) (e) (c) (f)

Fig. 7. (a) Hologram of several wires at two different positions, (b) reconstructed image of the two horizontal lines at the central part, and (c) reconstructed image taken by focusing on the other four lines. (d) Hologram of the same object with filtering on the two vertical lines, (e) reconstructed image focused on the two horizontal lines, and (f) reconstructed image focused on the other horizontal lines.

especially to the central hole diameter of the portion passing the zero-order spectrum.

We are now in a position to show the three-dimensional imaging properties of the in-line Fraunhofer hologram. Figure 7 (a) is the hologram of several straight wires at two different positions. Figure 7 (b) is a photograph of the reconstructed image of the two horizontal lines situated at the central part. Other lines are all out of focus in the photograph since it is only possible to focus one plane sharply at a time when we record the reconstructed image as a photograph. Figure 7 (c) is taken by focusing on the other four lines while the above two horizontal lines are now out of focus. Figure 7 (d) is the filtered hologram of the same object in which the two vertical lines are suppressed. Its reconstructed image is shown in Fig. 7 (e) in which the two horizontal lines are in focus while the other horizontal lines are out of focus and the two vertical lines are diminished. The reconstructed image of Fig. 7 (f) has a focus on the horizontal lines different from Fig. 7 (e). Thus we can see that the present in-line Fraunhofer holography has an ability of storing bubble tracks over a depth of field present in the actual bubble chamber dimensions.

5. Conclusion

The in-line filtered hologram presented here has many advantages. The resolution is very excellent, depending only upon the film used to record the hologram. Effects of the virtual image on the reconstructed image is almost completely negligible. Three-dimensional reconstruction of the bubblə chamber volume is also possible. The filtering process can be used at two stages, that is, the recording and reconstructing stages, although in the present experiment filtering was employed only at the recording stage. Diffused light can also be used to reduce the contrast of the hologram so that considerations on the linearities of the film used in the recording is not important[6].

Finally let us show that the present method is also useful in more complicated objects. Figure 8 (a) is the original object of words in three different characters. Figure 8 (b) is the hologram without filtering and Fig. 8 (c) the reconstructed imege. It can be pointed out from these figures that the present method has a high ability in reconstructing relatively complicated objects such as characters or line drawings although there are some limitations imposed by the far-field condition. Consequently, it is expected that the present holographic technique, which is fairly simple compared with the two beam interferometric method, will be applicable in the field of pattern recognition. Further study along this line is now being conducted and will be reported in the future.

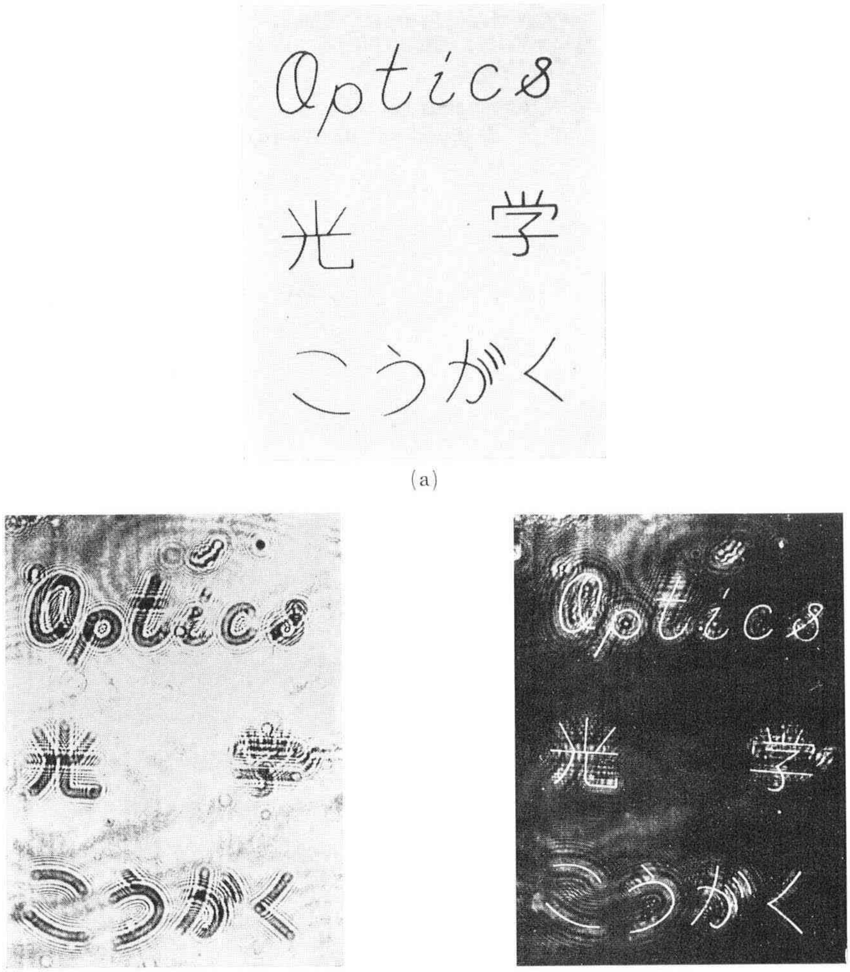

(a)

(b) (c)

Fig. 8. (a) Original object of the three different characters, (b) hologram without filtering, and (c) reconstructed image.

References

1) W. T. Welford: Appl. Opt. **5** (1966) 872.
2) J. H. Ward and B. J. Thompson: J. Opt. Soc. Am. **57** (1967) 275.
3) D. G. Falconer: Appl. Opt. **5** (1965) 1365.
4) G. B. Parrent and B. J. Thompson: Opt. Acta **11** (1964) 183.
B. J. Thompson: Japan. J. Appl. Phys. **4**, Suppl. 1 (1965). 302.
J. B. DeVelis, G. B. Parrent and B. J. Thompson: J. Opt. Soc. Am. **56** (1966) 423.

B. J. Thompson, J. H. Ward and W. R. Zinky: Appl. Opt. **6** (1967) 519.
G. O. Reynolds and J. B. DeVelis: IEEE Trans. **AP**-15 (1967) 41.
5) D. Gabor: Nature **161** (1948) 777.
D. Gabor: Proc. Roy. Soc. (London) **A 197** (1949) 454.
6) K. Murata, H. Fujiwara and T. Asakura: Japan. J. Appl. Phys. **7** (1968) 301.